Degredation Modeling and Remaining Useful Life Prediction of Electrolytic Capacitors under Thermal Overstress Condition Using Particle Filters

Hamed Khorasgani[1], Chetan Kulkarni[2], Gautam Biswas[3], José R. Celaya[4], and Kai Goebel[5]

[1,3] *Vanderbilt University, Nashville, TN, 37235, USA*
hamed.g.khorasgani@vanderbilt.edu
gautam.biswas@vanderbilt.edu

[2,4] *SGT Inc. NASA Ames Research Center, Moffett Field, CA, 94035, USA*
chetan.kulkarni@vanderbilt.edu
jose.r.celaya@nasa.gov

[5] *NASA Ames Research Center, Moffett Field, CA, 94035, USA*
kai.goebel@nasa.gov

ABSTRACT

Prognostic and remaining useful life (RUL) predictions for electrolytic capacitors under thermal overstress condition are investigated in this paper. In the first step, the degradation process is modeled as a physics of failure process. All of the relevant parameters and states of the capacitor are considered during the degradation process. A particle filter approach is utilized to derive the dynamic form of the degradation model and estimate the current state of capacitor health. This model is then used to get more accurate estimation of the Remaining Useful Life (RUL) of the capacitors as they are subjected to the thermal stress conditions. The paper includes an experimental study, where the degradation of a set of identical capacitors under thermal overstress conditions is studied to demonstrate and validate the performance of the degradation modeling approach.

1. INTRODUCTION

Prognostic and Remaining Useful Life (RUL) prediction is essential for determining the safety and reliability of critical systems. In the cases where the operators have access to the system RUL prediction, it becomes easier for them to establish condition-based maintenance schedules, and thus avoid failures and expensive system downtime. For autonomous systems, RUL prediction provides necessary information for the system to schedule future tasks and missions in an effective manner.

Electronic systems need reliable power supplies. Failure in the power supplies can damage other system elements through a cascading process. Many electronic modules are sensitive to the potential level of the supplied voltage and undesired change in this level can cause failure in these modules as well. Also unpredicted voltage variations can damage processors and make control modules in the systems unreliable. Switch mode power supplies (SMPS) can provide different voltage levels from a single power source by changing the duty cycle of switching. They are also efficient, light and have a small size. However the small size affects heat dissipation, and reliability becomes an important issue in these systems. Consequently RUL predictions for different elements of these systems are becoming increasingly important (Goebel et al., 2008; Celaya et al., 2010; Kulkarni et al., 2009). One of the key elements in power supply modules and dc-dc converters are electrolytic capacitors. Failures in these elements is one of main reasons for the module failures (Goodman et al., 2005). For the prognostic and RUL prediction of electrolytic capacitors like any other element in addition to the current state of the element, it is necessary to predict its future behavior. If we can determine and model the main reasons for the degradation of the capacitors, future behavior prediction becomes a feasible task.

Evaporation of the electrolyte is a main reason for the degradation and finally complete failure of the capacitor. In fact evaporation of the electrolyte decreases the effective surface area of the capacitors and consequently their capacitance. One of the complexities of this problem is that the evaporation

of the electrolyte in the closed can of the capacitor causes internal pressure increase, which affects the evaporation rate. It is also possible that due to the internal pressure the capacitor body pops exposing the electrolyte to the atmosphere. Under these circumstances, the capacitor electrolyte first shows abrupt increase in evaporation rate, but after its top pops, the evaporation rate becomes constant. Work on capacitor degradation modeling in (Celaya et al., 2012) considered the evaporation rate to be constant and derived the degradation model for electrolytic capacitors under electrical overstress condition. With this simplification, the derived model is linear and the authors could apply the Kalman filter scheme to estimate the current state of health of the system. In this paper, the evaporation rate is not held to a constant value. Two different degradation trajectories are considered: one for the situation where the capacitor casing remains perfect, therefore, the evaporation rate decreases with time, and a second when the casing cracks, therefore, the evaporation rate for the capacitor electrolyte remains constant. A general model is derived by combining these two models. Since the general derived degradation model is nonlinear, unlike (Celaya et al., 2012), we adopt the particle filter approaches (Arulampalam et al., 2002) for state estimation of the nonlinear dynamic system. The particle filter approach is also utilized to estimate parameters of the model for each capacitor. To determine the effectiveness and performance of the particle filter approach, we used experimental data generated in (Kulkarni et al., Sep 2012) to validate our approach.

The paper is structured as follows. Section 2 discusses the degradation processes and the physics of failure model corresponding to the degradation processes. Section 3 discusses the particle filter approach for state estimation in the prognostic algorithm. Particle filtering method for parameter estimation is discussed in this section as well. An algorithm for computing the RUL of the capacitor is presented as the last part of this section. Section 4 is about the experimental setup and parameter estimation. 15 electrolytic capacitors are studied under thermal over stress condition. The leave one out method is utilized to validate the parameters of the model and the derived model is used to make prognostic predictions. Section 5 demonstrates RUL prediction results and the conclusions are presented in Section 6.

2. DEGRADATION MODELING

Prognostics approaches start with the current state of a component or device and employ systematic methods to predict future system behavior. Having an accurate model of the degradation process provides a methodology for predicting future component behavior. In this section, the degradation model of the electrolytic capacitor is discussed and developed. We start with the structure of electrolytic capacitors and then discuss the degradation process. Last, a discretized form of the continuous degradation model is derived.

2.1. Electrolytic Capacitors Structure and Capacitance

If we open the aluminium can of an electrolytic capacitor we see the anode and cathode foils, and the electrolyte soaked in the separator paper all wrapped up together as shown in Figure 1. In the electrolytic capacitors that we study, ethyl glycol is the chosen electrolyte. The cathode and anode foils are aluminium. Also, the oxide layer on the surface of the anode acts as the dielectric. This oxide layer in contact with the electrolyte acts as a perfect insulator. By wrapping up the papers high capacitance is achieved in the minimum space.

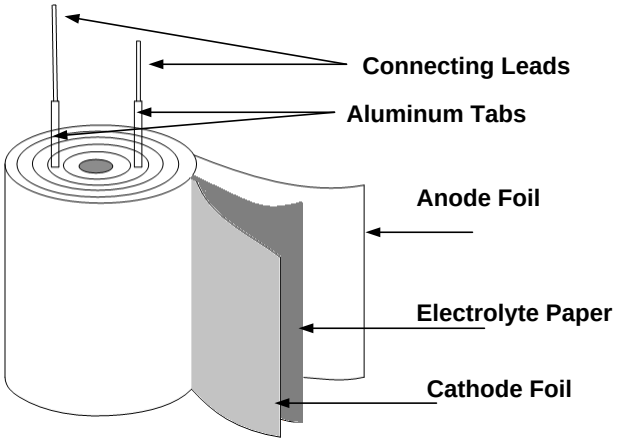

Figure 1. Cylindrical Electrolytic Capacitor Structure (Kulkarni et al., Sep 2012).

The capacity of the capacitance is defined in terms of its geometric structure. From the first principles of electromagnetism the total lumped capacitance of a flat plate electrolytic capacitor is:

$$C = \frac{\epsilon A}{d_o}, \tag{1}$$

where ϵ is dielectric constant of the electrolyte, A is the effective surface of the electrolyte and d_o is the oxide thickness. Rolling the plates of electrolytic capacitors double the capacitance of these capacitors (Tasca, 1981). This improvement achieves due to utilizing both sides of foils in the new structure. Consequently the capacitance of the presented structure in Figure 1 can be expressed as follows.

$$C = \frac{2\epsilon A}{d_o}. \tag{2}$$

Assuming that the separator paper thickness is negligible and the space between anode and cathode is completely filled by the electrolyte the volume of the electrolyte can be computed as:

$$V = A * d, \tag{3}$$

where d is the distance between anode and cathode foils. Therefore, the capacitance can be expressed based on elec-

trolyte volume by:

$$C = \frac{2\epsilon V}{d_o d}. \tag{4}$$

Equation (4) demonstrates how the evaporation of the electrolyte decreases the capacitance of the electrolytic capacitors. The electrolytic capacitor capacitance, C decreases directly in proportion to electrolyte volume, V, as it evaporates due to raised ambient temperatures. In the next section, we study the evaporation process for the electrolyte in greater detail.

2.2. Modeling Electrolyte Evaporation

The rate of evaporation and consequent decrease in the liquid volume depends on the surface area of the liquid, its molecular volume, and the evaporation rate (Rdner et al., 2002). So we can write:

$$\frac{dV}{dt} = -AJ\omega, \tag{5}$$

where A is the surface of electrolyte, J is the evaporation rate and ω is the volume of electrolyte (ethyl glycol) molecule. If we substitute A by $\frac{V}{d}$ in (5) we have:

$$\frac{dV}{dt} = -J\omega\frac{V}{d} \tag{6}$$

An important parameter in the derived equation is the evaporation rate. Typically the evaporation rate is not a constant parameter; it increases as the ambient temperature increases, therefore, the temperature at the capacitor core increases. In fact, if the molecules of electrolyte have more kinetic energy the probability that they leave the surface increases and consequently the evaporation rate increases. In our study, the ambient temperature in the experimental chamber is maintained constant. The other factor which affects the evaporation rate is pressure. Increasing the pressure at the surface of the liquid decreases the probability that molecules leave the surface, which means that the evaporation rate decreases. Further, a large pressure increase has other consequences, e.g., the top of the capacitor casing may pop. This releases all of the built up gases, bringing the surface pressure on the electrolyte surface back to the atmospheric pressure levels. We discuss the evaporation rates for two different scenarios: (1) capacitor casing not pierced, implying the inside of the capacitor is a closed system and (2) capacitor casing damaged and popped. $Capacitor\ as\ Closed\ System:$ As long as the capacitor casing is not pierced the capacitor is a closed system. In this situation, by evaporation the escaped molecules accumulate in the can and increase the pressure on the electrolyte surface. The increase in the pressure decreases the evaporation rate. The decrease in the evaporation rate continues and after some time it becomes so small that practically the evaporation stops. At this point the numbers of molecules which leave the liquid and return to it are almost the same and the vapor is said to be saturated. In the enclosed system, we use the exponential function to model the evaporation rate, i.e:

$$J = J_0 e^{-\beta t}, \tag{7}$$

where J_0 is the initial value of the evaporation rate which is function of temperature and density of the liquid. β determines how fast the evaporation rate decreases and depends on the volume of the enclosed space. $Open\ System\ with\ Capacitor\ Casing\ Pierced:$ The primary reason to covering the capacitors with an aluminum can is to protect the electrolyte from evaporation (Kulkarni et al., Jun 2012). However it is possible that a large increase in the internal pressure can pop or crack the cover in some way and the electrolyte escapes into to the atmosphere. When this happens, the evaporation rate after an initial increase becomes constant because the capacitor can is not a closed space anymore. In this case the evaporation rate is:

$$J = J_{open}, \tag{8}$$

where J_{open} depends on the temperature, atmosphere pressure and liquid concentration. As a next step we discuss the capacitor degradation model next.

2.3. State Space Model for Capacitance Degradation

To model capacitor degradation, a state space model with capacitance and evaporation rate as the state variables is considered. Using (4) one can write:

$$\frac{dC}{dt} = \frac{2\epsilon}{d_o d}\frac{dV}{dt}. \tag{9}$$

And by substituting (6) in (9) we have:

$$\frac{dC}{dt} = -2J\omega\epsilon\frac{V}{d_o d^2}. \tag{10}$$

Using (4) and doing some algebraic manipulations we can write:

$$\frac{dC}{dt} = -J\omega\frac{C}{d}. \tag{11}$$

For the enclosed case J can derived from (7) as:

$$\frac{dJ}{dt} = -\beta J_0 e^{-\beta t}. \tag{12}$$

By substituting (7) in (12) we have:

$$\frac{dJ}{dt} = -\beta J. \tag{13}$$

If the can cracks or pops up the evaporation rate is constant and the capacitance dynamic is:

$$\frac{dC}{dt} = -J_{open}\omega\frac{C}{d}. \tag{14}$$

2.4. Converting to Discrete-Time Model

Since measurements are sampled in discrete times we derive a discrete time model of the state space representation. Using a first-order approximation:

$$\frac{dC}{dt}(t_k) = \frac{C(t_{k+1}) - C(t_k)}{t_{k+1} - t_k}. \tag{15}$$

Consequently from (11) for the enclosed case we have:

$$C(t_{k+1}) = C(t_k) - J(t_k)\omega\frac{C(t_k)}{d}(t_{k+1} - t_k). \tag{16}$$

Similarly, using (13) the dynamic equation for J in enclosed space is derived as:

$$J(t_{k+1}) = J(t_k) - \beta J(t_k)(t_{k+1} - t_k). \tag{17}$$

Considering (14) for the capacitor case popped open we have:

$$C(t_{k+1}) = C(t_k) - J_{open}\omega\frac{C(t_k)}{d}(t_{k+1} - t_k) \tag{18}$$

2.5. General Model for the Degradation

An accurate model of capacitor degradation would use the enclosed degradation equation till the capacitor encasing popped, and at the popping time switch to the open model where the evaporation rate becomes constant. Since we do not know the exact time that the switch from the closed to open situation occurs, we employ a blended model that combines the enclosed and open degradation models, i.e.,

$$C = \alpha(t_k)C_{closed} + (1 - \alpha(t_k))C_{open}. \tag{19}$$

$\alpha(t_k)$ starts at a value close to 1.0 for t_k small, and gradually decrease as time advances. How the parameter α changes with time may be unknown, for the sake of simplicity we assume α decreases linearly with slope of c over time as represented by (20) . The value of c may be determined by empirical studies, or based on expert-supplied knowledge.

$$\alpha(t_{k+1}) = \begin{cases} \alpha(t_k) - c(t_{k+1} - t_k) & t_{k+1} \leq \frac{1}{c} \\ \\ \alpha(t_k) & t_{k+1} > \frac{1}{c}. \end{cases} \tag{20}$$

Therefore, an approximation of the capacitor degradation model can be expressed as:

$$\begin{aligned} C(t_{k+1}) = \alpha(t_k) * [C(t_k) - J(t_k)\omega\frac{C(t_k)}{d}(t_{k+1} - t_k)] + \\ (1 - \alpha(t_k)) * [C(t_k) - J_{open}\omega\frac{C(t_k)}{d}(t_{k+1} - t_k)] \\ J(t_{k+1}) = J(t_k) - \beta J(t_k)(t_{k+1} - t_k) \\ \alpha(t_{k+1}) = \begin{cases} \alpha(t_k) - c(t_{k+1} - t_k) & t_{k+1} \leq \frac{1}{c} \\ \\ \alpha(t_k) & t_{k+1} > \frac{1}{c}. \end{cases} \end{aligned} \tag{21}$$

3. PROGNOSTICS ALGORITHM

Using the degradation model we can design a filter to estimate the current state of health of the system. Using this estimated state of health and degradation model, we can predict the future behaviour of the capacitor and using end of life threshold we can estimate the remaining useful life. As discussed earlier, the degradation model includes three state variables that change with time, capacitance, C, evaporation rate, J and combination factor, α. Since we have run experiments and collected degradation data on a set of identical electrolytic capacitors, we can use our filter model in a predict-estimate-update loop to refine the degradation model as new measurements on the system become available. Applying the predict-estimate-update loop, we hypothesize that the estimation of RUL becomes more accurate as more data is obtained on capacitor degradation. Therefore, a combination of a model- and data-driven approach to prognostics will likely result in more accurate and general degradation models than if we employed pure data-driven methods (which don't generalize easily) and pure model-based approaches (which are hard to tune accurately without the availability of data).

Kalman filters have been proven to be optimal state estimators and predictors for linear time-invariant systems (Arulampalam et al., 2002). However, the state equations for capacitor degradation are nonlinear, therefore a Kalman filter approach will have to be approximated by extended Kalman filters (EKF). (Julier & Uhlmann , 1997) used EKF framework to develop unscented Kalman filters (UKF) which is another approximation of Kalman filters for state estimation in nonlinear systems. This method assume Gaussian distribution for the system states and utilizes a set of carefully chosen sample points, propagate them through the non-linear dynamic and uses the result to re-estimate the parameters of the Gaussian distribution in each step. These samples are chosen in a way to capture the exact mean and covariance of the Gaussian distribution completely and when propagate through the nonlinear dynamic capture the mean and covariance of the posterior distribution to the 3rd order Taylor series expansion approximation accurately. Since EKF uses first order Taylor series approximation it is expected that UKF exhibits better performance in the state estimation of nonlinear systems with Gaussian inputs (Wan & Van Der Merwe, 2000). In previous work, we have used unscented Kalman filters for state estimation and obtained fairly accurate degradation models and RUL estimates for both Electrical and Thermal overstress test conditions (Kulkarni, 2013). In this paper we adopt a more powerful approach to modeling and tracking non linear behavior evolution: the Particle filter that uses a sequential Monte Carlo approach for state estimation and does not assume Gaussian inputs for the system. Similar to EKF and UKF, Particle filter provides a suboptimal solution for the state estimation in nonlinear systems, however it is proved that by increasing the number of samples (particles) its so-

lution approaches the optimal Bayesian estimation (Arulampalam et al., 2002).

3.1. Particle Filter

In order to estimate the probability density distribution (pdf) of the state variables of a nonlinear system, the particle filter approach uses a set of particles (samples) and a set of associated weights representing the discrete probability masses of the particles. Particle Filter updates these particles and weights in each step to follow the evolution of the states of the dynamic system. In fact, particle filters use Monte Carlo method to implement a recursive Bayesian filter to estimate the pdf of the state variables. To implement particle filters, it is assumed that the dynamic system can be presented as a first order Markov process:

$$\begin{aligned} x_k &= f(x_{k-1}) + \omega_k \\ y_k &= h(x_k) + \upsilon_k, \end{aligned} \tag{22}$$

where x_k is the system states in step time k, y_k is the measurement and ω_k and υ_k represent system and sensor noises respectively.

Sequential Importance Sampling (SIS): SIS is an algorithm for implementing recursive filtering based on Monte Carlo method. The main idea is to approximate posterior density function $p(x_k|y_{1:k})$ by a set of random samples or particles $\{x_k^i\}_{i=1}^P$ and their associated weights $\{\omega_k^i\}_{i=1}^P$. As mentioned earlier as the number of these particles become very large the Monte Carlo characterization approaches to the posterior density function and SIS algorithm solution approaches the optimal Bayesian estimation.

$$\begin{aligned} p(x_k|y_{1:k}) \approx \sum_{i=1}^{P} w_k^i \delta(x_k - x_k^i) \\ \sum_{i=1}^{P} w_k^i = 1, \end{aligned} \tag{23}$$

where x_k^i are the particles and w_k^i are the normalized weights associated with them. These weights update based on importance distribution function $\pi(x_k|x_{0:k-1}, y_{1:k})$ in each step (Arulampalam et al., 2002) as follows :

$$w_k^i \propto w_{k-1}^i \frac{p(y_k|x_k^i)p(x_k^i|x_{k-1}^i)}{\pi(x_k^i|x_{0:k-1}^i, y_{1:k})}. \tag{24}$$

Degeneracy Problem and Resampling: Degeneracy problem happens when the variance of importance weights keep increasing over time and consequently after a certain number of step times most of the particles will have negligible importance weights. In this situation a fairly large percentage of computational effort would be devoted to update the weights associated with particles which have no meaningful contribution to the result. The degeneracy problem is not avoidable in SIS algorithm (Ristic et al., 2004). To overcome to this problem a resampling process is considered in each step time to replace the particles with low importance weight with particles which have higher importance weights. Resampling is a mapping from $\{x_k^i, \omega_k^i\}_{i=1}^P$ to $\{x_k^{i*}, \frac{1}{P}\}_{i=1}^P$ where new particles x_k^{i*} are chosen from the set of previous particles randomly with the probability equal to the importance weight of the particle so we have:

$$P\{x_k^{i*} = x_k^j\} = \omega_k^j. \tag{25}$$

Sampling Importance Resampling (SIR): By choosing importance distribution function equal to $p(x_k|x_{k-1})$, one can rewrite equation (24) as:

$$w_k^i \propto w_{k-1}^i p(y_k|x_k^i). \tag{26}$$

Also considering resampling procedure at each step time we assign $w_{k-1} = \frac{1}{P}$ for all the particle weights so we have:

$$w_k^i \propto p(y_k|x_k^i). \tag{27}$$

This filter is proposed by (Gordon et al., 1993) and is called SIR or bootstrap filter. To implement SIR filter we only need to know states space dynamic, measurements and noise model (22) and the likelihood function $p(y_k|x_k)$.

Particle Filters for Parameter Estimation: State estimation by particle filters is discussed in this section. Particle filters can be used for parameter estimation in nonlinear systems as well. The parameters do not change over time significantly so its dynamic in state space representation can be written as:

$$\begin{aligned} \rho_k &= \rho_{k-1} + \omega_k \\ y_k &= h(\rho_k, x_k) + \upsilon_k, \end{aligned} \tag{28}$$

where ρ represents system parameters and x is system states. ω and υ represents parameters uncertainty and sensor noise models respectively and y is the measurements. Based on our knowledge about the variance and expected value of the parameters we design ω_k and consider proper initial values for the parameters and the rest of the process is quit similar with state estimation procedure. Parameter estimation can be done simultaneously with state estimation or off line. In the off line scenario, we assume that the system states in different time steps are already measured and saved and we feed them as the inputs to equation (28) during the parameter estimation process. In the cases that states and parameters should be estimated simultaneously, parameters will be considered as the new states for the system and to calculate the value of the new states (which are the combination of original states and unknown parameters) in each time step we use the estimated value of them in previous time step as it was done in state estimation.

3.2. Remaining Useful Life Prediction

The particle filter estimates the current value of the capacitance considering the measurement values and the degrada-

tion model. It also updates the degradation model by providing a new value for evaporation rate and combination factor based on the measurement and the degradation model. To calculate the remaining useful life we use the current value of the capacitance as the initial value and the updated degradation model to predict the future behavior of the capacitor. Remaining useful life threshold is value provided by the factory which determines after a specific percentage of degradation in the capacitor the capacitor cant perform its normal function in the circuit. Having this value we can compare it with predicted capacitance of the electrolytic capacitor in future to estimate remaining useful life. The procedure is presented in figure 2.

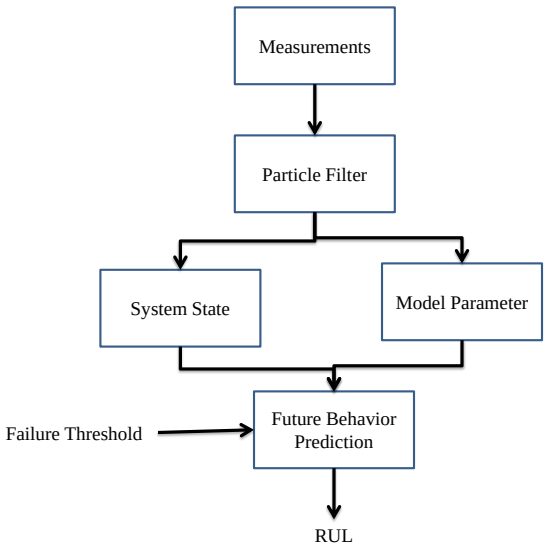

Figure 2. Prognostic flowchart.

4. SETUP AND MODEL ESTIMATION

In the first part of this section the experimental setup and the test conditions are presented. Then the parameters of the degradation method are estimated. Finally the remaining useful life prediction results are demonstrated and the performance of the algorithm is discussed.

4.1. Experimental Setup and Test Conditions

In order to present the performance of the proposed strategy for RUL prediction of the electrolytic capacitors 15 identical capacitors with $2200uF$ capacitance are utilized. The nominal working condition of the capacitance is $10V$ and 85^oC. The thermal over stress condition is provided by a temperature controlled chamber presented in figure 3. The capacitors were in 105^oC with 3.4% humidity factor for 3400 hours. And the capacitances of the capacitors were measured during the test regularly [13].

Figure 3. Thermal Chamber.

4.2. Parameters of the Degradation Model

In the derived degradation model for the electrolytic capacitor, thickness of electrolyte paper, d, can be measured for each class of capacitors after removing the cover. Volume of the electrolyte molecule is also a constant value that need to be determined based on the material used as the electrolyte. These parameters for the 15 identical capacitors that used in our case study are presented in Table 1. Dielectric constant, ϵ, was used in the modeling too, however since it did not appear in the final model for the degradation (21) we don't need to use it for RUL predictions.

There are also some other parameters in the degradation model which need to be determined in the prognostic design procedure. These unknown parameters as one can see in equation (21) are J_{open} , β and c. Also three initial conditions C_0 , J_0 and α_0 need to be determined. C_0 is considered equal to the nominal capacitance of each capacitor and J_0 is assumed equal to J_{open}. This approximation is not far away from reality because the internal pressure due to the evaporation is the main reason for decreasing J in the closed space and in the beginning there should not be significant evaporation. Finally α_0 is considered 1 because we assumed in the beginning of the thermal overstress test all the capacitors are healthy and non of the cans is not popped up. To estimate J_{open} , β and c for each capacitor the data associated with other 14 capacitors is considered and since the model is not linear, the particle filter scheme is applied for the estimation. The derived value for each capacitor is presented in Table 2. Figure 4 represents real degradation process and its corresponding degradation model for the first capacitor. It can be seen that the degradation model tracks real degradation process within an acceptable range of error. Mean square error between each capacitor's model derived by the parameters of Table 2 and its real degradation process is calculated by (29) and is presented in Table 3.

$$MSE = \frac{1}{n}\sum_{k=1}^{n}(C_{tk} - C'_{tk})^2, \tag{29}$$

where C_{tk} is the capacitance of the capacitor measured at time sample t_k and C'_{tk} is the value of capacitor obtained

Table 1. Parameter values of the degradation model

Parameter	Description	Value
d	Thickness of the electrolyte paper	$2.22 * 10^{-5} cm$
ω	Volume of ethyl glycol molecule	$5.66 * 10^{-9} cm^3$

Table 2. Parameter values of the degradation models

Capacitor	J_{open}	β	c
C_1	$0.2167 hr^{-1} cm^{-2}$	0.0041	0.0003
C_2	$0.2213\ hr^{-1} cm^{-2}$	0.0039	0.0003
C_3	$0.2183\ hr^{-1} cm^{-2}$	0.0029	0.0003
C_4	$0.1936\ hr^{-1} cm^{-2}$	0.0020	0.0003
C_5	$0.2232\ hr^{-1} cm^{-2}$	0.0029	0.0003
C_6	$0.2242\ hr^{-1} cm^{-2}$	0.0020	0.0003
C_7	$0.2177\ hr^{-1} cm^{-2}$	0.0042	0.0003
C_8	$0.2101\ hr^{-1} cm^{-2}$	0.0029	0.0003
C_9	$0.2076\ hr^{-1} cm^{-2}$	0.0033	0.0003
C_{10}	$0.2226\ hr^{-1} cm^{-2}$	0.0024	0.0003
C_{11}	$0.2186\ hr^{-1} cm^{-2}$	0.0028	0.0003
C_{12}	$0.2199\ hr^{-1} cm^{-2}$	0.0037	0.0003
C_{13}	$0.2211\ hr^{-1} cm^{-2}$	0.0038	0.0003
C_{14}	$0.2034\ hr^{-1} cm^{-2}$	0.0027	0.0003
C_{15}	$0.2180\ hr^{-1} cm^{-2}$	0.0026	0.0003

Table 3. Mean square errors for the capacitors models

Capacitor	mse
C_1	1.0e-08 * 0.0637
C_2	1.0e-08 *0.1069
C_3	1.0e-08 *0.0149
C_4	1.0e-08 *0.0379
C_5	1.0e-08 *0.0732
C_6	1.0e-08 *0.0482
C_7	1.0e-08 *0.0968
C_8	1.0e-08 *0.2286
C_9	1.0e-08 *0.0476
C_{10}	1.0e-08 * 0.0649
C_{11}	1.0e-08 *0.1447
C_{12}	1.0e-08 * 0.0258
C_{13}	1.0e-08 *0.1237
C_{14}	1.0e-08 *0.0204
C_{15}	1.0e-08 * 0.1958

from its degradation model at the same time. It should be mentioned here that in the prognostic procedure system states like J and α update during the process as the system measure the capacitance of the capacitor in each step. So it is expected that in the prognostic simulation the model demonstrates even better tracking performance.

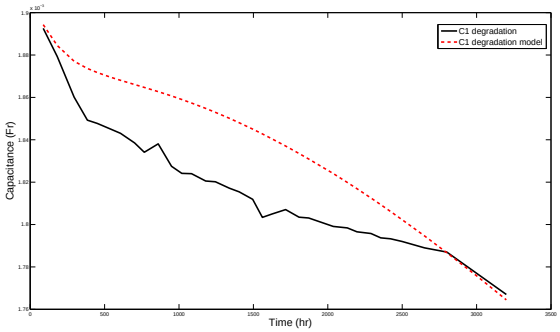

Figure 4. Degradation models.

5. Experimental Results

Using the proposed degradation model and the estimated variables, the remained useful life prediction for the capacitors are done according to the proposed methodology in section 3. The remaining useful life is considered when the capacitance of the capacitor decreases below 90% of its nominal value (Kulkarni et al., Sep 2012). Also in designing the particle filter 300000 sample points were considered. Figure 5 shows the actual remaining useful life and the estimated remaining useful life of the first capacitor from the beginning of the thermal overstress test to the end of its useful life. One can see from the this figure that by getting closer to the end of life of the capacitor the error of the prediction decreases and the predicted value converges to the real value of RUL. To explain this observation we can say as the system gets more data and the particle filter updates the degradation model, the degradation model becomes closer to the real degradation procedure and the predicted RUL based on the degradation model becomes more exact.

The RUL prediction relative accuracy (RA) is defined as:

$$RA = 100(1 - \frac{\mid RUL - RUL_e \mid}{RUL}) \qquad (30)$$

where RUL is the remained useful life and RUL_e is the estimated remaining useful life. relative accuracy of the prediction of remaining useful life for each capacitor in each step time is presented in Table 3. The results show the prediction method is completely reliable and relative accuracy is improved in comparison with the previous works.

Table 4. Relative Accuracy

time(hr)	C_1	C_2	C_3	C_4	C_5	C_6	C_7	C_8	C_9	C_{10}	C_{11}	C_{12}	C_{13}	C_{14}	C_{15}
87.7	91.14	79.98	98.72	98.1	90.89	86.46	93.15	78.9	98.1	82.41	85.99	86.17	98.45	95.25	67.41
181.7	87.14	84.49	96.51	95.15	91.2	79.88	92.48	74.61	96.88	81.4	84.32	87.58	96.13	94.36	70.96
295.4	78.56	90.57	95.76	94.58	94.51	81.62	99.23	85.42	93.33	82.68	86.34	86.55	97.88	92.7	74.9
384.5	89.59	90.58	94.44	96.03	95.56	79.59	96.76	85.42	91.19	83.45	91.34	88.02	92.54	95.92	73.55
450.9	89.46	87.17	95.35	95.70	95.15	82.4	99.42	88.12	94.31	85.11	91.92	87.69	94.2	99.63	75.82
540.8	91.79	83.73	92.48	98.22	95.36	84.57	99.61	84.95	93.29	84.72	88.54	87.04	96.84	99.8	76.97
607.1	94.94	88.82	95.37	95.82	93.65	85.16	97.69	84.12	94.46	83.56	87.36	89.41	94.58	99.7	77.12
701.6	96.5	86.47	94.29	92.43	97.66	87.59	99.34	82.25	93.08	85.29	90.63	86.59	93.78	97.73	74.4
766.8	97.76	81.34	93.27	96.55	93.27	85.19	95.1	81.34	98.65	79.03	88.56	89.11	96.21	98.35	72.66
860.4	94.93	79.47	96.22	91.42	99.06	92.53	94.66	85.86	90.66	87.55	94.66	83.86	92.75	93.11	77.81
950.1	99.22	89.18	97.09	90.73	98.94	93.07	92.98	83.44	87.02	93.3	92.98	84.68	92.57	91.01	76.84
1019	94.49	95.01	97.1	87.82	96.38	94.11	91.37	85.04	86.83	94.16	91.28	83.24	92.64	91.56	71.56
1084.5	89.63	98.09	94.7	87.89	95.91	93.34	92.1	85.02	87.3	93.68	89.03	80.07	92.69	90.76	71.41
1179.5	86.15	89.25	95.8	87.05	98.76	92.28	92.52	81.8	86.69	93.87	88.7	79.27	94.67	93.54	73.36
1244.8	96.77	94.21	98.08	85.77	96.62	91.39	92.65	82.21	87.92	92.9	90.8	76.86	92.06	92	72.16
1338.2	94.96	97.24	97.22	82.98	93	90.33	92.45	82.48	87.16	91.78	87.94	74.74	92.73	92.39	73.24
1404.5	83.71	98.63	92.53	84.53	95.56	86.48	93.62	81.84	92.1	85.95	84.89	78.55	95.44	93.68	75.86
1495.4	75.2	92.83	92.79	76.24	88.31	93.07	86.67	91	82.64	93.81	94.78	68.98	84.53	82.58	86.43
1560.5	93.04	97.17	99.08	71.81	85.98	95.19	84.65	93.48	77.15	95.77	95.26	65.9	85.09	81.28	91.19
1626.5	86.49	91	90.16	79.74	89.58	93.01	90.39	93.69	79.81	93.28	90.52	67.07	87.83	83.72	89.1
1716.6	96.27	92	94.62	71.14	84.71	97.12	87.07	90.8	75.95	97.34	97.19	65.61	84.49	78.32	90.37
1807.0	86.95	96	93.79	76.18	86.19	89.94	88.83	93.47	77.61	98.29	95.43	67.3	86.79	82.88	87.98
1871.6	91.48	83.05	99.78	72.04	84.6	93.04	89.32	98.89	76.17	95.28	94.24	64.3	85.37	81.41	80.92
2036.9	78.98	82.07	99.89	79.16	89.64	87.98	94.79	93.13	82.81	95.75	91.07	68.31	92.82	82.06	82.56
2131.3	86.56	84.77	97.01	77.79	88.35	91.02	90.04	93.71	79.98	98.39	93.51	64.94	87.35	75	82.55
2196.1	87.15	95.84	92.53	77.04	92.21	97.15	95.39	87.45	87.59	92.4	84.38	67.92	96.49	81.98	73.49
2290.1	97.75	85.9	96.9	72.62	94.42	92.17	98.69	90.64	82.22	91.35	85.31	69.42	93	81.63	81.63
2356	88.42	79.3	79	74.92	90.73	80.19	98.96	93.56	82.51	95.87	99.21	65.41	88.42	65.28	87.28
2421.9	95	63	89.81	72.42	88.42	77.28	98.28	86.71	78.28	88.42	87.14	51.57	80.28	60.28	92.57
2500	94.55	61	84.75	75.27	90.72	74.72	96.54	83.81	78.36	91.09	82.72	44.9	81.63	59.81	99.09
2650	97.5	69.25	59.5	81.5	83.5	67.75	93.5	85	68.5	88.75	78.25	60.5	82.5	48.75	96.75
2800	100	97	100	64.5	86	74.5	84	80	87.5	88	76.5	86	84	54	93

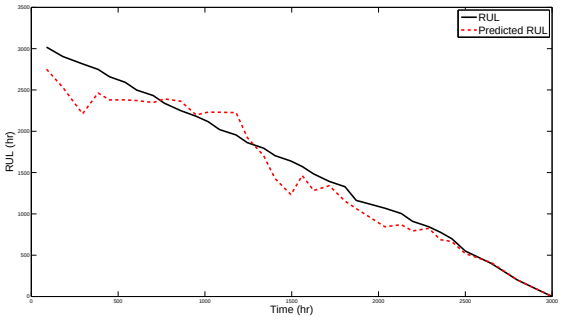

Figure 5. RUL Estimation.

6. CONCLUSION

In this paper a general model with three state variables is considered to represent the degradation process of the electrolytic capacitors. There is no doubt that degradation process is a nonlinear complex phenomenon. To perform prognostics with high performance and acceptable range of error we had to take in to account these nonlinearities in the degradation model. The results of experimental study shows acceptable performance in relative accuracy of RUL predictions. However, by adding these complexities to the model the number of parameters we have to estimate for the model increased as well. This can be a potential problem in designing a remaining useful life predictor model. In the estimation of each capacitor's model parameters we did not use that capacitor's data. In fact we considered 14 other capacitors to estimate its parameters. So we can claim that derived values for the system parameters can be used for any similar capacitor and we expect to get acceptable results as well. One of the advan-

tages of this work is as the system comes close to the failure, the performance of RUL prediction improves. The reason of this observation is discussed in the paper but it has an important practical value. In fact from the safety and mission critical point of view it is much more important for the operators to have an exact estimation of RUL when we are close to the end of life or failure.

In this paper degradation of the electrolytic capacitors under thermal over stress condition is studied. However, the suggested degradation model and prognostic algorithm can be applied for RUL prediction of a capacitor under electrical overstress condition as well. In fact, in electrical overstress condition because of additional chemical reactions in the capacitors (Gmez-Aleixandre et al., 1986), capacitor popping is more likely, making this model more relevant. In future work, we will apply the suggested degradation model and prognostic method for RUL prediction of electrolytic capacitors under electrical overstress condition.

REFERENCES

Arulampalam, M. S., Maskell, S., Gordon, N., Clapp, T. (2002). A tutorial on particle filters for online nonlinear/non-Gaussian Bayesian tracking. Signal Processing, IEEE Transactions on, 50(2), 174-188.

Celaya, J. R., Wysocki, P., Vashchenko, V., Saha, S., Goebel, K. (2010, September). Accelerated aging system for prognostics of power semiconductor devices. In AUTOTESTCON, 2010 IEEE (pp. 1-6). IEEE.

Celaya, J. R., Kulkarni, C. S., Biswas, G., Goebel, K. (2012). Towards A Model-based Prognostics Methodology for Electrolytic Capacitors: A Case Study Based on Electrical Overstress Accelerated Aging. International Journal of Prognostics and Health Management.

Gmez-Aleixandre, C., Albella, J. M., Martnez-Duart, J. M. (1986). Pressure build-up in aluminium electrolytic capacitors under stressed voltage conditions. Journal of applied electrochemistry, 16(1), 109-115.

Goebel, K., Saha, B., Saxena, A., Celaya, J., Christophersen, J. (2008). Prognostics in battery health management. Instrumentation and Measurement Magazine, IEEE, 11(4), 33-40.

Goodman, D. L., Vermeire, B., Spuhler, P., Venkatramani, H. (2005, March). Practical application of PHM/prognostics to COTS power converters. In Aerospace Conference, 2005 IEEE (pp. 3573-3578). IEEE.

Gordon, N. J., Salmond, D. J., Smith, A. F. (1993). Novel approach to nonlinear/non-Gaussian Bayesian state estimation. In IEE Proceedings F (Radar and Signal Processing) (Vol. 140, No. 2, pp. 107-113). IET Digital Library.

Julier, S. J., Uhlmann, J. K. (1997, July). New extension of the Kalman filter to nonlinear systems. In AeroSense'97 (pp. 182-193). International Society for Optics and Photonics.

Kulkarni, C., Biswas, G., Koutsoukos, X. (2009, October). A prognosis case study for electrolytic capacitor degradation in DC-DC converters. In PHM Conference.

Kulkarni, C. S., Celaya, J. R., Biswas, G., Goebel, K. (2012, June). Physics based Modeling and Prognostics of Electrolytic Capacitors. Aerospace 2012, 19-21 June, Garden Grove, California.

Kulkarni, C. S., Celaya, J. R., Goebel, K., Biswas, G. (2012, September). Bayesian Framework Approach for Prognostic Studies in Electrolytic Capacitor under Thermal Overstress Conditions.

Kulkarni, C. S. (2013). A Physics-based Degradation Modeling Framework for Diagnostic and Prognostic Studies in Electrolytic Capacitors (Doctoral dissertation, Vanderbilt University).

Rdner, S. C., Wedin, P., Bergstrm, L. (2002). Effect of electrolyte and evaporation rate on the structural features of dried silica monolayer films. Langmuir, 18(24), 9327-9333.

Ristic, B., Arulampalm, S., Gordon, N. J. (2004). Beyond the Kalman filter: Particle filters for tracking applications. Artech House Publishers.

Tasca, D. M. (1981, September). Pulse power response and damage characteristics of capacitors. In EOS/ESD Symposium Proceedings. Las Vegas: ESD Assn, Rome, NY (pp. 174-91).

Wan, E. A., Van Der Merwe, R. (2000). The unscented Kalman filter for nonlinear estimation. In Adaptive Systems for Signal Processing, Communications, and Control Symposium 2000. AS-SPCC. The IEEE 2000 (pp. 153-158). IEEE.

Hamed Khorasgani is a Ph.D candidate at ISIS, Vanderbilt University, Nashville, TN. He received the M.S.c degree in Mechatronics Engineering, in 2012 from Amirkabir University of Technology, Iran and a B. Sc. in Electronics and Electrical Engineering in 2009 from Isfahan University of Technology, Iran.

Chetan S. Kulkarni received the B.E. (Bachelor of Engineering) degree in Electronics and Electrical Engineering from University of Pune, India in 2002 and the M.S. and Ph.D. degrees in Electrical Engineering from Vanderbilt University, Nashville, TN, in 2009 and 2013, respectively. In 2002 he joined Honeywell Automation India Limited (HAIL) as a Project Engineer. From May 2006 to August 2007 he was a Research Fellow at the Indian Institute of Technology (IIT) Bombay with the Department of Electrical Engineering. From Aug 2007 to Dec 2012, he was a Graduate Research Assistant with the Institute for Software Integrated Systems and Department of Electrical Engineering and Computer Science, Vanderbilt University, Nashville, TN. Since Jan 2013 he is

Research Engineer II with SGT Inc. at the Prognostics Center of Excellence, NASA Ames Research Center. His current research interests include physics-based modeling, model-based diagnosis and prognosis focused towards electrical and electronic devices and systems. Dr. Kulkarni is a member of the Prognostics and Health Management (PHM) Society, AIAA and the IEEE.

Gautam Biswas received the Ph.D. degree in computer science from Michigan State University, East Lansing. He is a Professor of Computer Science and Computer Engineering in the Department of Electrical Engineering and Computer Science, Vanderbilt University, Nashville, TN. His primary research interests are in modeling and simulation of complex, hybrid systems, fault diagnosis and prognostics, and fault-adaptive control. His research has been supported by DARPA, NASA, and NSF. He has over 400 refereed publications.

José R. Celaya is a research scientist with SGT Inc. at the Prognostics Center of Excellence, NASA Ames Research Center. He received a Ph.D. degree in Decision Sciences and Engineering Systems in 2008, a M. E. degree in Operations Research and Statistics in 2008, a M. S. degree in Electrical Engineering in 2003, all from Rensselaer Polytechnic Institute, Troy New York; and a B. S. in Cybernetics Engineering in 2001 from CETYS University, México.

Kai Goebel received the degree of Diplom-Ingenieur from the Technische Universitt Mnchen, Germany in 1990. He received the M.S. and Ph.D. from the University of California at Berkeley in 1993 and 1996, respectively. Dr. Goebel is a senior scientist at NASA Ames Research Center where he leads the Diagnostics and Prognostics groups in the Intelligent Systems division. In addition, he directs the Prognostics Center of Excellence and he is the technical lead for Prognostics and Decision Making of NASAs System-wide Safety and Assurance Technologies Program. He worked at General Electrics Corporate Research Center in Niskayuna, NY from 1997 to 2006 as a senior research scientist. He has carried out applied research in the areas of artificial intelligence, soft computing, and information fusion. His research interest lies in advancing these techniques for real time monitoring, diagnostics, and prognostics. He holds 15 patents and has published more than 200 papers in the area of systems health management.